Nanoscale Systems for Optical Quantum Technologies

Grant Agreement No: 712721
Start Date: 1st October 2016 - Duration: 36 months

D1.6 Magnetic field effects on Eu^{3+}

Deliverable:	D1.6
Work package:	WP1 Nanomaterials, optical micro-cavities and control systems
Task:	1.1 Y_2O_3 nanoparticles development
Lead beneficiary:	CNRS
Type:	Report
Dissemination level:	Public
Due date:	30 September 2019
Actual submission date:	30 September 2019
Author(s):	D. Serrano, P. Goldner (CNRS-CP)

This project has received funding from the European Union's Horizon 2020 research and innovation programme under grant agreement No 712721.

Version history

Version	Date	Author(s)	Description
V1	23/09/2019	D. Serrano (CNRS-CP)	First draft
V2	28/09/2019	D. Serrano, P. Goldner (CNRS-CP)	Revised manuscript
V3	30/09/2019	D. Serrano, P. Goldner (CNRS-CP)	Submission to EC

Table of Contents

Deliverable Description

In this deliverable, we investigate optical homogeneous linewidths from a small number of nanoparticles. For this, we perform fluorescence detection based spectral hole burning using a cryogenic optical microscopy configuration. Spectral hole widths and hole decay times are recorded in the presence and absence of external magnetic fields. Limitations of the experimental approach employed here are discussed. We finally expose future perspectives for the study of coherent phenomena in single nanoparticles.

Introduction

Important progress has been achieved during NanOQTech in the experimental measurement of rare-earth nanoparticle's optical and spin homogeneous linewidths [1-5]. These achievements are due to the particle's good coherence properties, maintained even when decreasing the average particle size down to 60 nm [2], but also to the optimization of the experimental technique used for detecting photon and spin echoes from ensembles of particles [6]. Although very efficient, this ensemble approach presents, however, several drawbacks. In particular, particle ensembles provoke strong scattering of the optical excitation pulses, preventing accurate control over Rabi frequencies. As a consequence, pulse errors have been shown to reduce the efficiency of spin coherence lifetime extension protocols such as all-optical dynamical decoupling [4]. The randomly oriented particles in the ensemble also limit the use of external magnetic fields to reduce decoherence [7]. Finally, the ensemble measurements produce average values of parameters, whereas single particles will be used in WP2 micro-cavity based demonstrations. For all these reasons, it is necessary to develop linewidths measurement and coherence control at the single-particle level. This will be an important first step towards using rare-earth doped nanoparticles for optical quantum technologies applications.

An important challenge in the single particle approach is the reduced number of available rare-earth emitters. As an example, the number of expected fluorescence counts at the detector are given in **Figure 1**, for particles doped with 0.3% Eu^{3+} and taking into account standard experimental conditions in our setup.

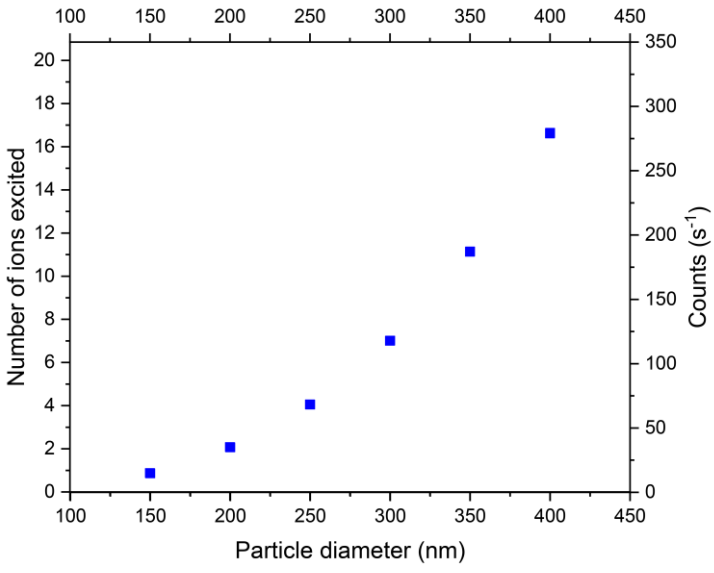

Figure 1: *Number of ions excited and expected count rate at the detector for a single Eu^{3+} doped nanoparticle (0.3% at.) as a function of particle diameter. The calculation considers known experimental values for our setup. The laser has a line width of 200 kHz and excites only 0.002% of the Eu^{3+} optical inhomogeneous line in Y_2O_3. The total collection efficiency is estimated at ~3%.*

A very promising strategy to work with single rare-earth nanoparticles, and even down to the single-ion level is, as mentioned, intensively investigated in NanOQTech's WP2: **Spin-atom-photon interfaces**, consisting of coupling the particles to fiber-based optical micro-cavities [8]. In the absence of cavity coupling, the investigation of single rare-earth doped nanoparticles requires combining scannable micron-scale spatial resolution with ultra-high collection efficiency in a cryogenic environment. In the present report, we describe how we developed such a setup and how we attempted using fluorescence-detection based spectral hole burning (SHB) to investigate homogeneous linewidths from a small number of nanoparticles deposited on a bulk Y_2SiO_5 crystal. The effect of applying an external magnetic field is also discussed.

Methods

Sample preparation

A batch of Eu^{3+}: Y_2O_3 nanoparticles with 400 nm average diameter and 0.3% doping concentration was synthesized following the standard homogeneous precipitation route described in previous works (see D1.2 and D1.3 for more details). 5 mg of the dried powders were then diluted into 0.5 ml of ethanol. A drop of the mix was deposited over the polished surface of an undoped Y_2SiO_5 crystal (5×4×1.55 mm) and left to dry. The resulting sample is shown in **Figure 2a**. Large aggregates of particles can be observed on the crystal surface. A second and more diluted sample was prepared by adding a lower number of particles in the initial mix (<1 mg in 0.5 ml ethanol). As in the previous case, a drop of the mix was deposited on the polished surface of a bulk Y_2SiO_5 crystal (1.5×3×0.6 mm) and left to dry. This home-grown substrate was chosen to eliminate background fluorescence. As it can be observed in **Figure 2b,** particles are hardly distinguishable on the crystal surface in this case.

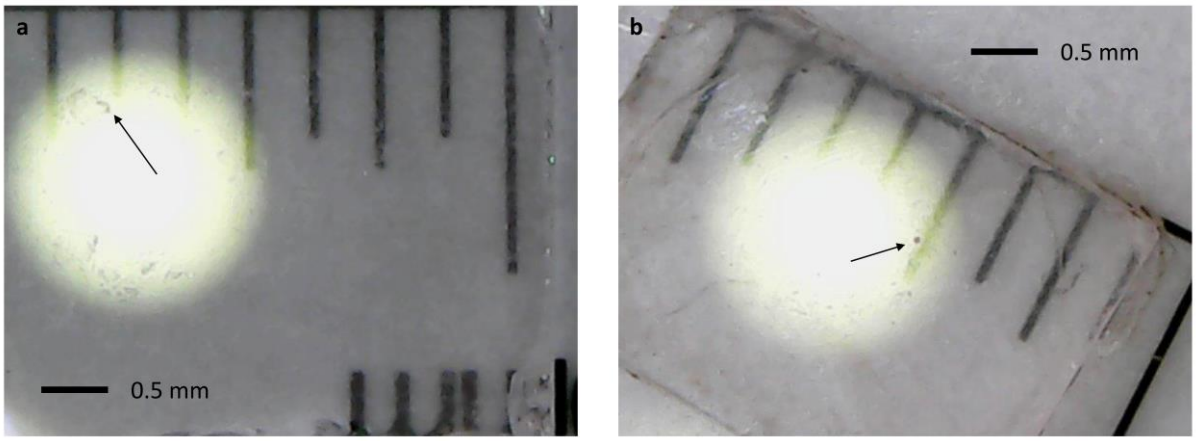

Figure 2: *Optical microscopy image of the samples.* ***a.*** *Sample "1",* ***b.*** *Sample "2".*

Experimental setup and pulse sequence

The spectroscopic measurements were carried out with a home-built cryogenic microscopy setup (**Figure 3**). This setup is a modified version of the one used in Ref. [8]**.** Excitation at 580.8830 nm ($^7F_0$ → $^5D_0$ transition) is performed using a tunable dye laser with 200 kHz linewidth (Sirah Matisse DS). To create the SHB pulse sequences, the cw

laser output is modulated by a double pass acousto-optic modulator (AOM) with a central frequency of 200 MHz driven by an arbitrary waveform generator (AWG). The modulated beam is then coupled to a polarization-maintaining single-mode optical fiber and the collimated fiber output is sent through a low transmission / high reflection beam splitter (10:90). The beam splitter was chosen with such high reflection and low transmission characteristics to maximize collection while limiting the incident excitation power.

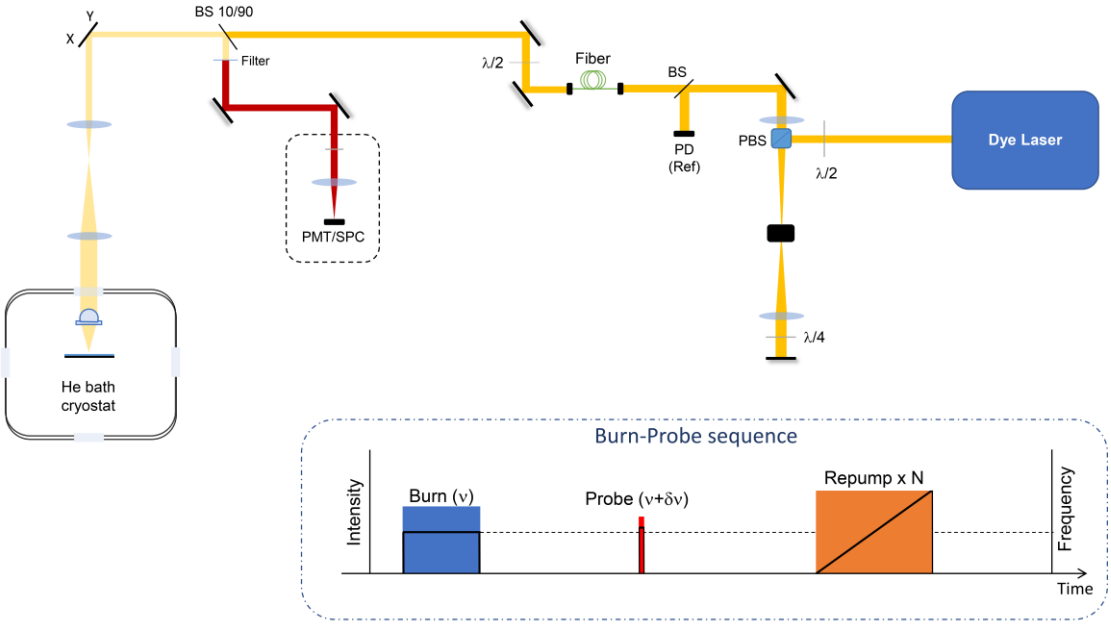

***Figure 3**: Experimental setup. **Inset:** burn-probe sequence.*

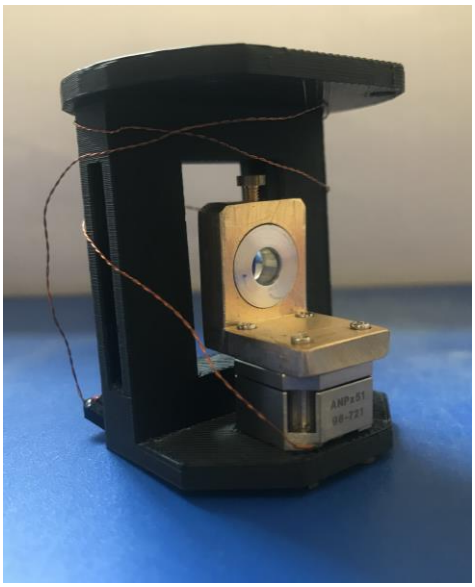

***Figure 4**: Home-built intra-cryostat assembly containing the nano-positioner and focusing lens.*

After the beam splitter, and before reaching the cryostat's optical window, the excitation beam is reflected by a movable mirror followed by two lenses forming a 4f system. This setting is used to scan the laser beam over the substrate crystal surface and select particles. Focal distances in the 4f setting were tightly adjusted to obtain an effective scan range of 50×50 μm. The minimum step size was set to 500 nm. Inside the He bath cryostat

(Janis SVT), focusing of the excitation beam into the sample and collection was done by an aspheric lens with 0.78 numerical aperture and 3.1 mm focal length. The lens position with respect to the sample was adjusted using an Attocube nano-positioner. A specific part, shown in **Figure 4**, was designed to hold sample, lens, and positioner within the He bath. Fluorescence detection was carried out by a high-sensitivity photomultiplier tube (PMT Hamamatsu R10699). The temperature was kept at 2 K during the measurements. Several fluorescence filters were used along the collection path to reject the excitation wavelength and isolate fluorescence.

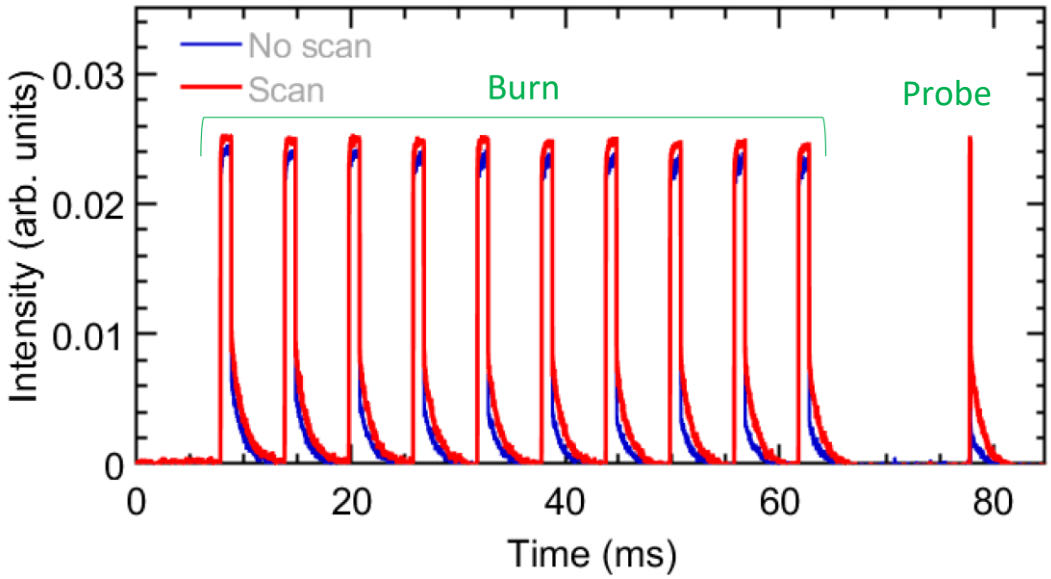

***Figure 5**: Example of a burn-probe sequence composed of 10 burning pulses (1 ms long and fixed frequency) and a single probe pulse (50 µs long). Waiting times were set to 3 ms between burning pulses and to 15 ms between burn and probe. The optical burning process is evidenced when the laser frequency is not scanned (blue trace): a progressive decrease in the maximal fluorescence intensity is observed just after the end of each burning pulse, and very clearly after the probe pulse. When the laser frequency is scanned (red trace), hole burning does not occur and the fluorescence is constant and stronger than in the previous case.*

Once signal from Eu^{3+}: Y_2O_3 nanoparticles on the crystal surface was identified, we carried out a series of fluorescence-detection based SHB experiments as a first approach to investigate optical homogeneous linewidths of few particles as a function of the magnetic field. The sequence used is shown in **Figure 3(inset)** and an experimental example is given in **Figure 5**. As it can be seen, the sequence is composed of a series of burning pulses followed by a single probe pulse. The creation of a spectral hole is evidenced by the variations in fluorescence intensity after the probe pulse in presence and absence of laser frequency scanning, which effectively turns on and off spectral hole burning. The hole width can be then measured by observing the variation of fluorescence emission intensity when detuning the probe pulse frequency with respect to the burning pulses.

Results and discussion

Spectral holes obtained from sample 1 are displayed in **Figure 6**, presenting a full width at half maximum (FWHM) of about Γ_{hole} = 2.8 MHz. This gives an upper limit for the optical homogeneous linewidth ($\Gamma_h = \Gamma_{hole}/2-\Gamma_{laser}$) in the MHz range, which is about an order of

magnitude larger than the homogeneous linewidth (106 kHz) obtained by two-pulse photon echoes for the same batch of nanoparticles. The choice of a different spatial spot, i.e. another group of particles, yielded similar results suggesting that the discrepancy is not related to variations from particles to particles. We note that important differences between homogeneous linewidths derived from two-pulse photon echoes and fluorescence-detection based spectral hole burning were also observed in [9] when studying a bulk Y_2SiO_5: Eu^{3+} crystal. This points to an experimental bias in the SHB measurements that has not been clearly explained up to now. No effect in the hole width was observed under external magnetic field. The spectral hole obtained for B = 28 G is also shown in **Figure 6**, for comparison with the zero-field hole.

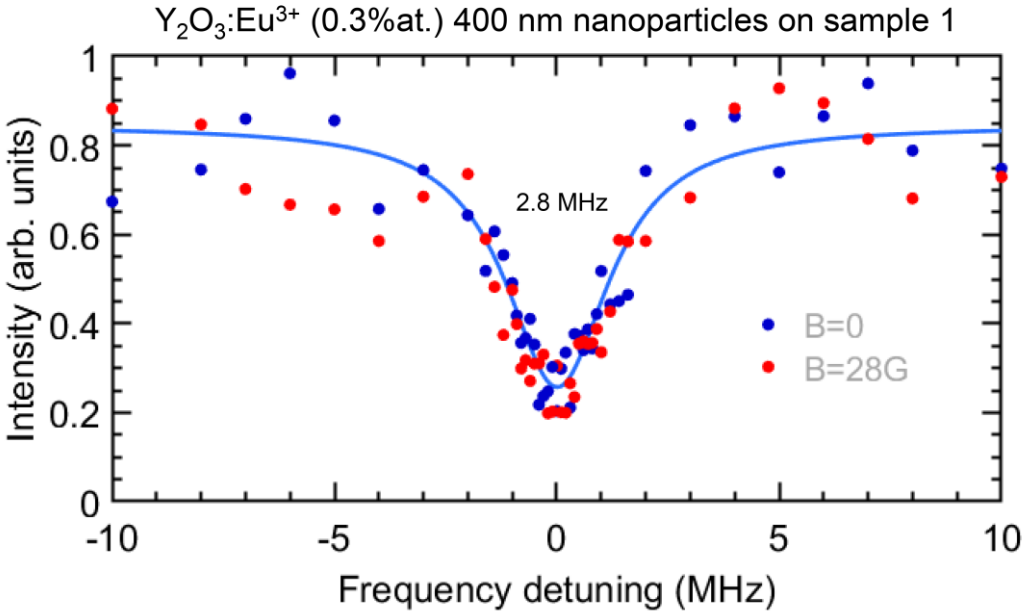

***Figure 6**: Spectral holes obtained from sample 1, at zero applied magnetic field (blue dots) and for B =28 G (red dots). A hole width of the order to 2.8 MHz FWHM is obtained in both cases.*

In the aim of limiting the experimentally induced hole broadening, we characterized the evolution of the spectral hole depth as a function of the burning pulse length, (**Fig. 7a**), and as a function of the number of pulses (**Fig. 7b**) using sample 2. It was found that a single burning pulse, with a length of 100 μs, was indeed enough to create detectable spectral holes. In view of these results, spectral hole line widths were measured again from particles on sample 2 under two different experimental conditions: first using a single burning pulse, and second applying 5 burning pulses (**Figure 8**). Unexpectedly, very similar hole widths were measured in both cases, and comparable to those given in **Figure 6**, for 10 burning pulses. From this, we concluded that reducing the total sequence length from ~100 ms (as in **Fig. 5**) to about 5 ms does not reduce the hole width, which suggests that power broadening nor spectra diffusion (on ms time scales) are responsible for the difference between SHB and photon echoes.

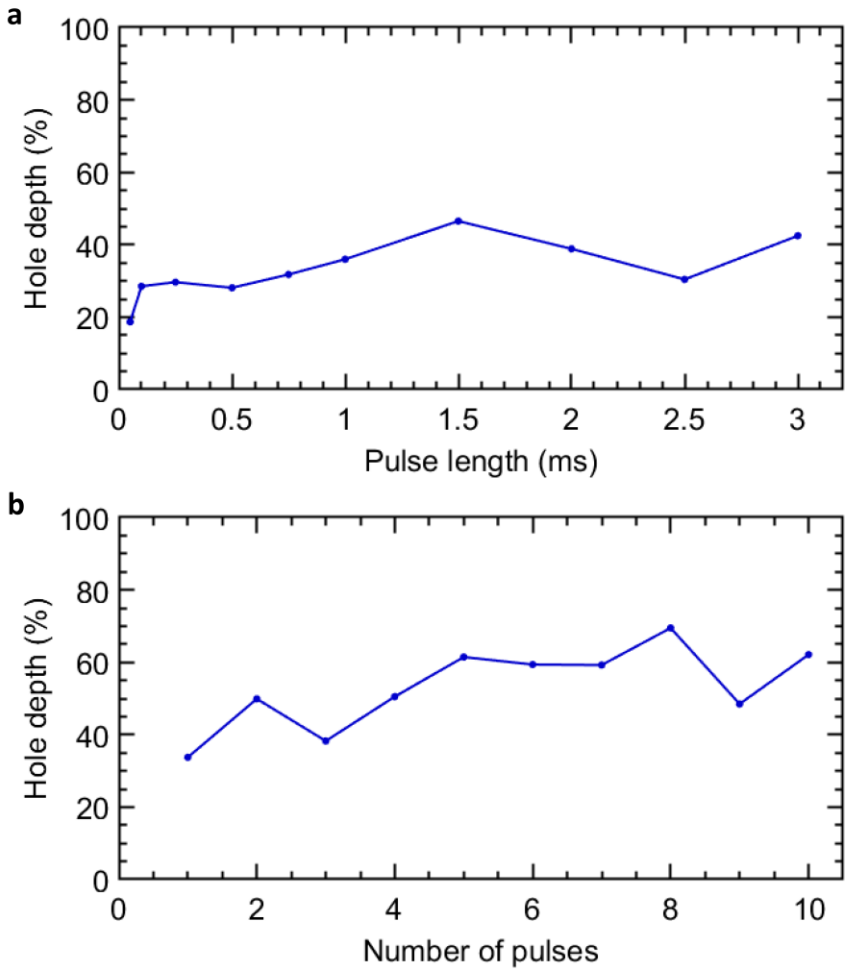

***Figure 7**: **a.** Hole depth as a function of burning pulse length. **b.** Hole depth as a function of number of burning pulses for a fixed pulse length of 1 ms. Data obtained from sample 2 at B=0.*

Fluorescence based spectral hole burning appears as an efficient approach to create and detect spectral holes even with a low number of emitters (estimated < 100 in the case of sample 2). Nevertheless, it leads to broad spectral holes and further understanding of this effect is needed before optical homogeneous linewidths from single nanoparticles can be reliably estimated by this method.

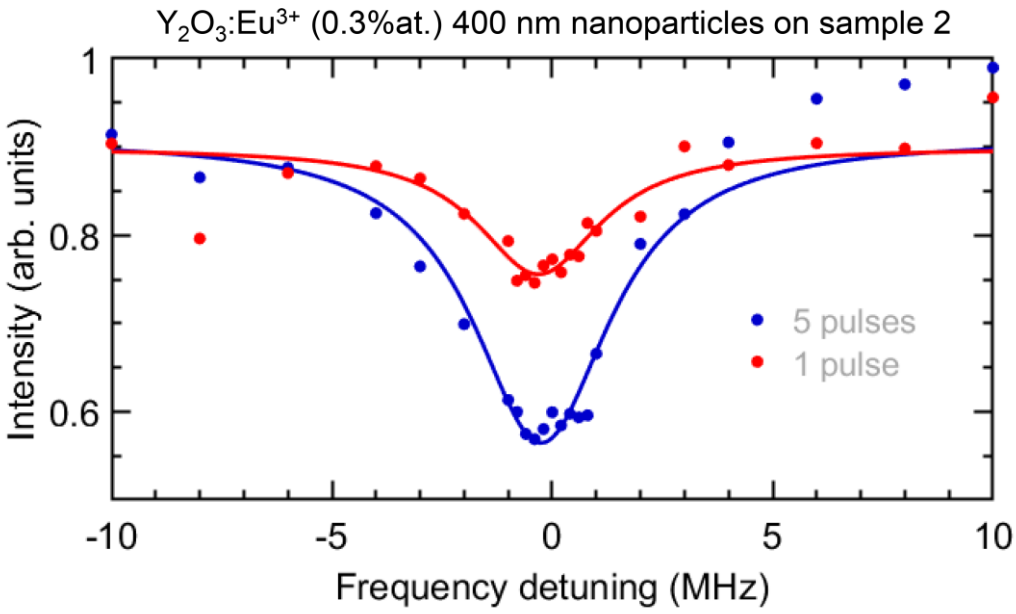

***Figure 8**: Spectral holes measured from sample 2 under two different conditions: with a single burning pulse (blue), and with a sequence of 5 burning pulses (red). A shallow hole is obtained when using the short sequence although this does not lead to a narrower hole width. B=0 in all cases.*

We finally measured hole decays as a function of waiting time between the last burning pulse and the probe pulse (**Figure 9**), with and without external magnetic field. A fast decay time constant of ~ 500 ms is obtained, roughly estimated given the large experimental error for long burn-probe delays. The presence of a slow component is also observed although it could not be reliably quantified as long delays (> 2 s) could not be probed with the current sequence implementation. As in the hole linewidth measurements, no clear difference was observed in the presence of an external field.

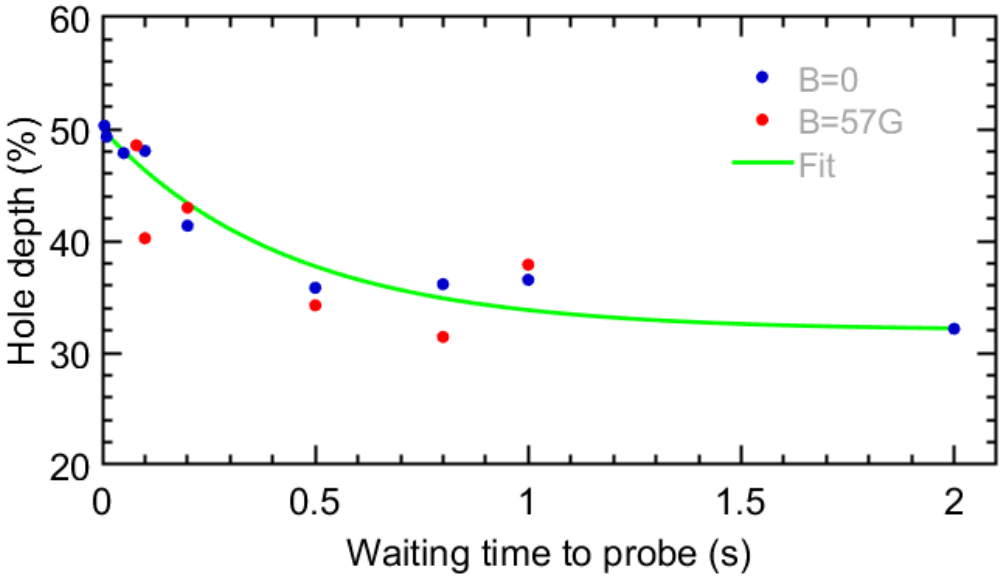

***Figure 9**: Hole depth as a function of waiting time between burn and probe pulses.*

Perspectives

Based on the measured signal to noise ratios, the current setup collection and detection efficiencies seem sufficient for studying isolated single particles of 400 nm. Smaller sizes, especially below 200 nm, could however be challenging unless a single photon detector is used for these low light level measurements (**Figure 1**). Furthermore, more accurate sample preparation by techniques such as spin coating will also be used to ensure better particle dispersion. Additional fluorescence-based SHB experiments will be performed to better understand the broadening mechanisms. Single crystals will be especially useful in this respect since they can show sub-kHz optical homogeneous linewidths with very low spectral diffusion over long times.

Conclusion

We have detected spectral holes from small numbers of Y_2O_3: Eu^{3+} particles deposited on bulk Y_2SiO_5 by using a home-built cryogenic microscopy setup. Hole widths of the order of 3 MHz and hole lifetimes of about 500 ms (fast component) were obtained. External magnetic fields of a few 10s of Gauss had no effect on hole widths nor lifetimes. These results open the way to further studies of narrow optical homogeneous linewidths in single rare-earth doped nanoparticles. An important point to clarify, however, is the additional broadening observed using fluorescence based SHB compared to photon echo experiments on ensembles of particles.

References

[1] D1.3: *Optical linewidth and spin T_2 in Eu^{3+}: Y_2O_3 particles.*
[2] D1.4: *Optimized nanoparticles and thin films.*
[3] S. Liu, D. Serrano, A. Fossati, A. Tallaire, A. Ferrier, P. Goldner, RCS Advances 8, 7098 (2018).
[4] D. Serrano, J. Karlsson, A. Fossati, A. Ferrier, P. Goldner, Nat. Commun. 9, 2127 (2018).
[5] J. G. Bartholomew, K.l de Oliveira Lima, A. Ferrier, P. Goldner, Nano Lett. 17, 778 (2017).
[6] A. Perrot, Ph. Goldner, D. Giaume, M. Lovric,C. Andriamiadamanana, R. R. Gonçalves and A. Ferrier, Phys. Rev. Lett. 111, 203601 (2013).
[7] D. L. McAusland, J. G. Bartholomew, M. J. Sellars and J. J. Longdell, Phys. Rev. A 85 032339 (2012).
[8] B. Casabone, J. Benedikter, T. Hümmer, F. Oehl, K. de Oliveira Lima, T. W. Hänsch, A. Ferrier, P. Goldner, H. de Riedmatten, D. Hunger, New J. Phys. 20 (2018).
[9] D3.5: *Comparison between FIB samples and thin films for nanoresonators.*